DOI: 10.1002/cmdc.201100314

Asymmetric Synthesis and Conformational Analysis by NMR Spectroscopy and MD of Aba- and α-MeAba-Containing Dermorphin Analogues

Bart Vandormael,[a] Rien De Wachter,[a] José C. Martins,[b] Pieter M. S. Hendrickx,[b] Attila Keresztes,[c] Steven Ballet,[a] Jayapal R. Mallareddy,[c] Fanni Tóth,[c] Géza Tóth,[c] and Dirk Tourwé*[a]

Dermorphin analogues, containing a (*S*)- and (*R*)-4-amino-1,2,4,5-tetrahydro-2-benzazepin-3-one scaffold (Aba) and the α-methylated analogues as conformationally constrained phenylalanines, were prepared. Asymmetric phase-transfer catalysis was unable to provide the (*S*)-α-Me-*o*-cyanophenylalanine precursor for (*S*)-α-MeAba in acceptable enantiomeric purity. However, by using a Schöllkopf chiral auxiliary, this intermediate was obtained in 88% *ee*. [(*S*)-Aba 3-Gly 4]dermorphin retained μ-opioid affinity but displayed an increased δ-affinity. The corresponding *R* epimer was considerably less potent. In contrast, the [(*R*)-α-MeAba 3-Gly 4]dermorphin isomer was more potent than its *S* epimer. Tar-MD simulations of both non-methylated [Aba 3-Gly 4]dermorphin analogues showed a degree of folding at the C-terminal residues toward the N terminus of the peptide, without however, adopting a stabilized β-turn conformation. The α-methylated analogues, on the other hand, exhibited a type I/I′ β-turn conformation over the α-MeAba 3 and Gly 4 residues, which was stabilized by a hydrogen bond involving Tyr 5-H_N and D-Ala 2-CO.

Introduction

Three types of opioid receptors, μ, δ and κ, have been identified. These receptors are involved in pain perception, regulation of mood, reward, motivation and response to stress.[1] They can be activated by endogenous opioid peptides or exogenously administered opiates, which act as analgesic drugs for moderate to severe pain. It is well known that the chronic use of common opioid analgesics results in the development of analgesic tolerance.[2] Therefore, the search for new strong analgesics with suppressed adverse side effects and abuse potential is still ongoing. Conformational, topographical and stereoelectronic structural features of the opioid peptides are important for interaction with the μ, δ, and κ opioid receptors.[3]

The heptapeptide dermorphin, H-Tyr-D-Ala-Phe-Gly-Tyr-Pro-Ser-NH_2 (**1**) was isolated from the skin of the South American frog *Phyllomedusa Sauvagei*.[4] It is one of the most potent and selective μ-opioid receptor agonists among naturally occurring opioids.[5] The minimal sequence required for opiate-like activity in vivo was identified as the N-terminal tetrapeptide.[6] It was shown by NMR analysis and X-ray studies that the optimal message domain for both μ and δ opioid receptors is the tripeptide Tyr 1-D-Ala 2-Phe 3 in a β-turn conformation. This turn conformation is induced by the D-chirality of the second residue.[7,8] A general feature of opioid peptides containing the Tyr 1-D-Xaa 2-Phe 3 message domain, was the unusually high-field position (<1 ppm) of the side chain protons of the second residue in the ^{1}H NMR spectra. This is observed for dermorphin,[9] its analogues[7] and in the δ-selective heptapeptide deltorphin.[10,11] Thus, a common preferred solution conformation of the N-terminal tripeptide was proposed to be a type I/I′ β-turn conformation around Xaa 2-Phe 3 in which the side chain of the second residue is "sandwiched" between the aromatic rings of Tyr 1 and Phe 3.[9,12–16] The μ/δ selectivity was mainly attributed to the conformation and polarity of the C terminus.[12] In addition, conformational restrictions in the flexibility of the peptide side chains of Tyr 1 and Phe 3 in dermorphin, and short dermorphin analogues, have been shown to cause shifts in selectivity and affinity.[17–19]

The 4-amino-1,2,4,5-tetrahydro-2-benzazepin-3-one scaffold (Aba; Figure 1) is able to fix the side chain orientation of the Phe 3 residue into the *trans* ($\chi_1 = 180^\circ$) or *gauche*(+) ($\chi_1 = 60^\circ$) staggered conformation.[17,18] The incorporation of the conformationally constrained dipeptide, Aba-Gly, (**2**) in positions 3 and 4 of dermorphin, resulted in a major increase in δ affinity with substantial loss of selectivity.[18,19] In contrast, the Tic structure **3** (Figure 1) is able to fix the *gauche*(+) and *gauche*(−) conformations, but excludes the *trans* conformation of the Phe

[a] Dr. B. Vandormael, Dr. R. De Wachter, Prof. S. Ballet, Prof. D. Tourwé
Department of Organic Chemistry, Vrije Universiteit Brussel
Pleinlaan 2, 1050 Brussels (Belgium)
E-mail: datourwe@vub.ac.be

[b] Prof. J. C. Martins, Dr. P. M. S. Hendrickx
Organic Chemistry Department, Universiteit Gent
Krijgslaan 281S4, 9000 Ghent (Belgium)

[c] Dr. A. Keresztes, J. R. Mallareddy, Dr. F. Tóth, Prof. G. Tóth
Biological Research Center
Temesvári Körút 62, 6701 Szeged (Hungary)

Supporting information for this article is available on the WWW under http://dx.doi.org/10.1002/cmdc.201100314.

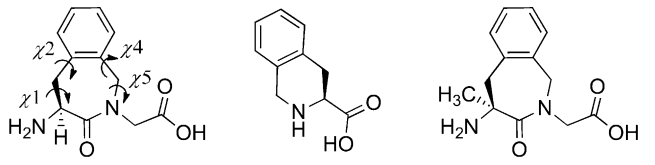

Figure 1. Structures of the conformationally constrained Phe analogues and definition of the dihedral angles.

side chain. Since a profound decrease in μ- and δ affinity and activity can be observed for the [Tic 3]dermorphin analogue,[17] it has been speculated that the bioactive conformer at the δ opioid receptor binding site is likely to be the *trans* rotamer of Phe.[17]

It was shown by both molecular modeling and NMR analysis that Aba 3 adopts the *trans* conformation ($\chi_1 = 180^\circ$) in [Aba 3-Gly 4]dermorphin-NH_2 (**5**).[17] We have previously reported that

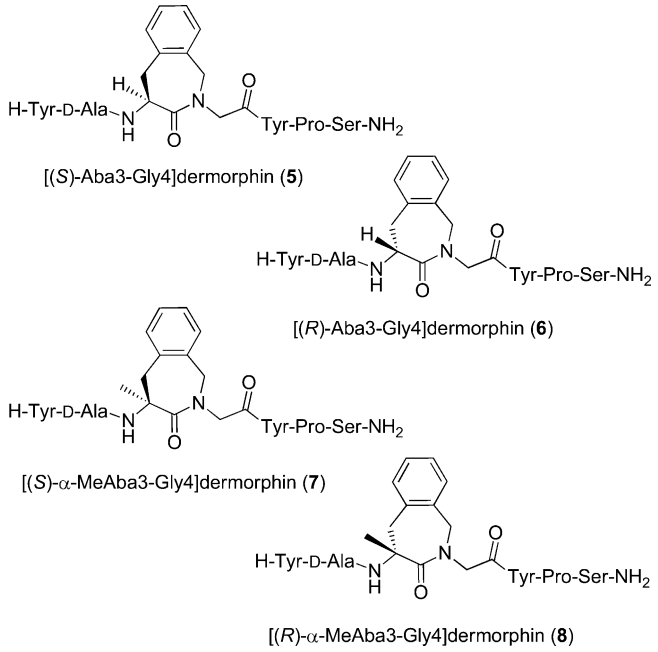

the Aba-Gly structure adopts a chair-like ring conformation, but is not able to induce a turn structure in the Ac-Aba-Gly-NHMe model.[20] In contrast, the α-Me-substituted Aba analogue adopts a boat-like ring conformation, and was shown to be a strong β-turn inducer in this model.[21] This is an analogy to the finding that α-MePro is a stronger turn inducer than Pro.[22,23]

Herein we compare the effects of *S* and *R* stereoisomers of Aba and α-MeAba incorporated into the dermorphin sequence on μ- and δ-opioid receptor affinity, functionality and on the conformation of the dermorphin analogues. Whereas asymmetric synthesis of Aba-Gly has been described,[18–20] only a racemic synthesis of α-MeAba-Gly was reported.[21] We now also describe the asymmetric variant of the latter.

Results and Discussion

Synthesis

The synthesis of Boc-(*S*)- and Boc-(*R*)-Aba-Gly-OH was performed starting from phthaloyl-protected (*S*)-Phe-Gly and (*R*)-Phe-Gly, respectively, by using a *N*-acyliminium ion cyclization, as described earlier.[17,19] Both enantiomers were incorporated into the dermorphin sequence to give **5** and **6** by standard solid phase peptide synthesis by using Boc chemistry and 4-methyl-benzhydrylamine (MBHA) resin as solid support. Racemic Boc-α-MeAba-Gly was prepared starting from (*R*,*S*)-α-Me-*o*-cyanophenylalanine, as described earlier.[21] After incorporation into the dermorphin sequence, the resulting peptide epimers, **7** and **8**, were separated by semipreparative RP-HPLC. In order to assign the absolute configuration of these [α-MeAba 3]-containing epimers, asymmetric synthesis of α-MeAba-Gly was performed. Since (*R*,*S*)-α-Me-*o*-cyanophenylalanine was conveniently obtained by phase-transfer catalyzed (PTC) alkylation of *N*-benzylidene alanine ethyl ester with *o*-cyanobenzyl bromide,[21] and since we obtained *o*-cyanophenylalanine with high enantiomeric purity using a cinchonidinium-based chiral phase-transfer catalyst,[20] this method was our first choice for the asymmetric synthesis of α-MeAba (Scheme 1).

Numerous methods have already been reported for the asymmetric synthesis of mono-alkylated α-amino acids from prochiral protected glycine derivatives by PTC alkylation with a chiral quaternary ammonium salt as catalyst.[24–30] In a pioneering work, O'Donnell et al. described the asymmetric synthesis of α-methyl-α-amino acids through enantioselective phase-transfer alkylation of the *p*-chlorobenzaldimine of (*S*)-alanine *tert*-butyl ester **9a** with enantiomeric excesses up to only 50%.[31]

By using the more efficient *N*-antracenylmethyl dihydrocinchonidium bromide catalyst **19** Lygo et al. improved the enantioselectivity for the preparation of α-MePhe to 87%.[32] More

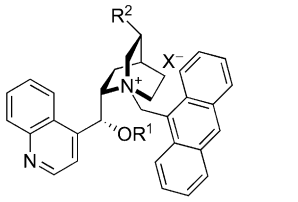

19: R^1 = H; R^2 = CH_2–CH_3; X = Cl
20: R^1 = H; R^2 = CH=CH_2; X = Cl
21: R^1 = Allyl; R^2 = CH_2–CH_3; X = Br

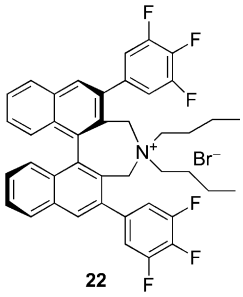

22

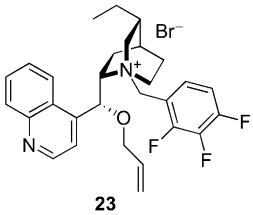

23

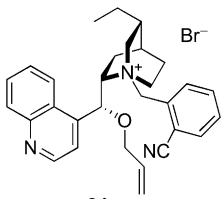

24

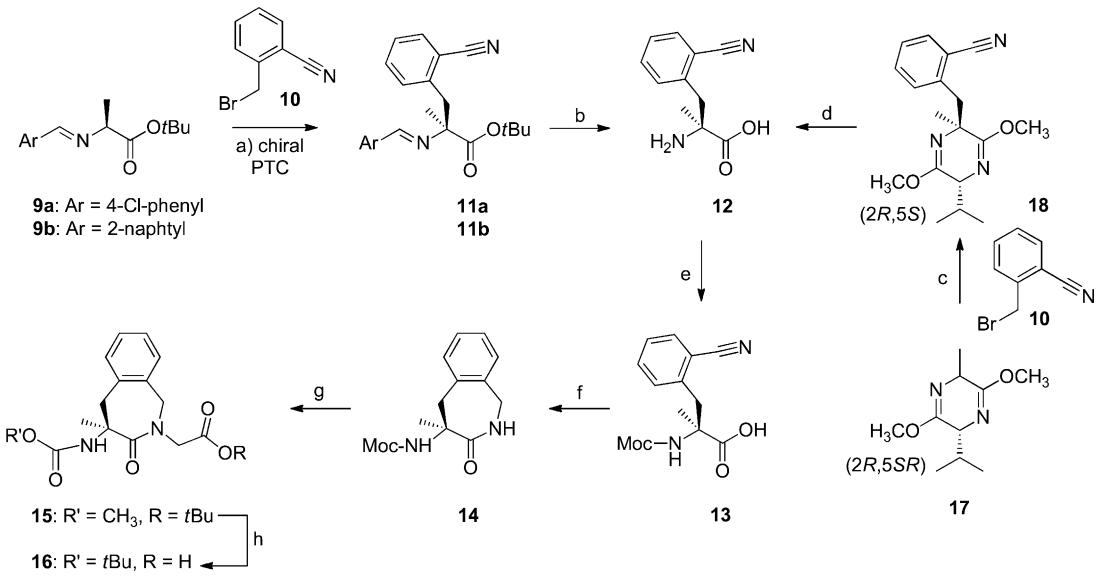

Scheme 1. Asymmetric synthesis of Boc-(*S*)-α-MeAba-Gly-OH (**16**). Conditions: a) see Table 1; b) TFA/H_2O (95:5), room temperature, overnight; c) *tert*-BuLi (1.6 M), dry THF, Ar, −78 °C, 1 h, *o*-CN-BnBr, 10 h (72%); d) i) TFA AcN/water (3:1), room temperature, overnight (quantitative), ii) HCl (6 N), 65 °C, 50 h (65%); e) NaOH (1 N), MocCl, 1 h (70%); f) i) Pd/C, H_2, EtOH/water, AcOH (10%), 0.34 mpa, 48 h, room temperature (85%), ii) EDC, pyridine, AcN/H_2O (3:1), room temperature, overnight (87%); g) NaH, DMF, $BrCH_2COOtBu$, 1 h, room temperature (47%); h) i) HBr (33%) in AcOH, 55 °C, 1.5 h, and ii) Boc_2O, Et_3N, dioxane/water (9:1), room temperature, overnight (67%).

recently, Chinchilla and colleagues optimized the reaction conditions for the benzylation of **9a** using catalyst **20**. When the 2-naphthyl aldimine **9b** was used instead of imine **9a**, the *ee* increased from 82 to 87%.[33] A C_2-symmetric non-Cinchona phase-transfer catalyst, derived from (*S*)-binaphthol, was used by the Maruoka group for the benzylation of **9a**, with an enantioselectivity of 98%.[34,35]

With catalyst **22**, which is also commercially available, the Maruoka group obtained the same enantioselectivity (98%) for this reaction.[36] Jew et al. reported on the synthesis of α-alkyl alanines by phase-transfer alkylation of the 2-naphthyl aldimine *tert*-butyl ester **9b** with RbOH and *O*(9)-allyl-*N*-2′,3′,4′-trifluorobenzylhydrocinchonidinium bromide (**23**) as a catalyst, with up to 96% *ee*.[37] Catalyst **23** and the *N*(1)-2′-cyanobenzyl derivative **24** were also successfully applied to the synthesis of α-amino acids with enantioselectivities varying from 94 to >99% *ee*.[38,39]

We have investigated the alkylation of aldimines **9a** and **9b** with *o*-cyanobenzyl bromide (**10**; Scheme 1) using various chiral catalysts and conditions described for the reaction with benzyl bromide. The results are shown in Table 1.

First, the third generation catalyst of Corey et al.,[26,29] **21**, was used for the enantioselective catalytic phase-transfer alkylation of the *p*-chlorobenzaldimine of alanine *tert*-butyl ester **9a** with CsOH as a base at −78 °C. These conditions were already proven to yield (*S*)-*o*-cyanophenylalanine in our laboratory with an enantioselectivity of 96%.[20] However, a considerably lower *ee* was obtained for the alkylation of the alanine derivative (Table 1, entry 1, 40% *ee*). We, therefore, changed to the third generation Cinchona catalyst of Lygo et al.,[28] **20**, and used the 2-naphthyl aldimine alanine *tert*-butyl ester **9b**, as described by Chincilla et al.[33] However, this procedure did not improve the enantioselectivity (Table 1, entry 2, 36% *ee*). In accordance with the results reported by Jew and co-workers, the aldimine **9a**, RbOH and *O*(9)-allyl-*N*-1-cyanobenzylhydrocinchonidinium bromide (**24**)[39] catalyst were used in the alkylation reaction, but only a moderate *ee* of 60% was obtained (Table 1, entry 3).

Table 1. Enantioselective catalytic phase-transfer alkylation of **9a** or **9b** with *o*-cyanobenzyl bromide under specified conditions.

Entry	Aldimine	Catalyst	Base	*T* [°C]	*t* [h]	Solvent	*ee*[a] [%]
1	**9a**	**21**	CsOH	−78	27	CH_2Cl_2	40
2	**9b**	**20**	RbOH	−20	24	toluene/$CHCl_3$ (7:3)	36
3	**9a**	**24**	RbOH	−35	26	toluene/CH_2Cl_2 (5:2)	60
4	**9a**	**23**	RbOH	−35	26	toluene	54
5	**9a**	**24**	RbOH	−78	20	toluene/CH_2Cl_2 (5:2)	13
6	**9a**	**24**	CsOH	−35	4	toluene	68
7	**9b**	**24**	RbOH	−35	21	toluene/CH_2Cl_2 (5:2)	34
8	**9b**	**23**	RbOH	−35	21	toluene/CH_2Cl_2 (5:2)	58
9	**9a**	**24**	CsOH	−35	4	CH_2Cl_2	60
10	**9a**	**23**	CsOH	−35	4	CH_2Cl_2	70
11	**9b**	**22**	CsOH	−20 °C	1	toluene	40

[a] Enantiomeric purity was determined by HPLC analysis after hydrolysis of **11a**,**b** to **12** and (*S*)-NIFE derivatization.[40]

Switching to the *O*(9)-allyl-*N*-2′,3′,4′-trifluorobenzylhydrocinchonidinium bromide catalyst (**23**),[37,38] under the same reaction conditions, did not improve the enantioselectivity (entry 4, 54% *ee*). Lowering the temperature to −78 °C (entry 5, 13% *ee*), switching to CsOH as a base (entry 6, 68% *ee*) by using the 2-naphthyl aldimine **9b** (entry 7, 34% *ee*) or/and another catalyst (entry 8, 58% *ee*) did not improve the enantioselectivity dramatically in comparison with entry 3. The use of only CH_2Cl_2 as a solvent in the enantioselective alkylation also did not lead to further improvements (entry 9, 60% *ee*; entry 10, 70% *ee*). Finally, the commercially available catalyst used by the Maruoka group, **22**,[36] was applied in the phase-transfer catalysis reaction of **9b** with *o*-cyanobenzyl bromide. Unfortunately, this did also not improve the enantioselectivity (entry 11, 40% *ee*). These experiments demonstrate that the *o*-cyano substituent drastically lowers the obtained enantiomeric excess, compared to those obtained for alkylations by using unsubstituted benzyl bromide. Therefore, another asymmetric synthesis method for α-Me-*o*-cyanophenylalanine (**12**) had to be chosen.

Fortunately, various other methodologies for the asymmetric synthesis of quaternary α-amino acids have been reported. These include Schöllkopf's bis-lactim ether strategy,[41,42] Williams' diphenyloxazinones method,[43] and Seebach's oxazolidinone-based methodology,[44] or one of its variants.[45–50] By using an optimized Schöllkopf protocol, as described by Vassiliou et al.,[51] (*S*)-α-Me-*o*-CN-Phe·HCl (**12**) was synthesized with good enantioselectivity (Scheme 1).

Deprotonation of the substituted bis-lactim ether chiral auxiliary **17** with *t*BuLi, followed by an alkylation of the resulting anion with *o*-cyanobenzyl bromide (**10**) provided compound **18** with a yield of 72% after purification by flash column chromatography. Hydrolysis of **18** by using TFA at room temperature, and subsequent hydrolysis of the methyl ester in HCl (6 N) at 65 °C, yielded (*S*)-α-Me-*o*-CN-Phe·HCl (**12**) with an *ee* of 88%, as determined by HPLC analysis after (*S*)-NIFE derivatization[40] (*S*)-α-Me-*o*-CN-Phe·HCl was methyloxycarbonyl (Moc)-protected to **13** by means of MocCl, as previously described for the racemic compound.[21] Reduction of the nitrile in **13** with H_2/Pd on C provided the aminomethyl derivative, which underwent intramolecular cyclization to **14** after activation of the carboxylic acid by using *N*-(3-methylaminopropyl)-*N*-ethylcarbodiimide (EDC). *N*-Alkylation of Moc-(*S*)-α-MeAba (**14**) with *t*Bu-bromoacetate and NaH as a base provided the ester **15**. Moc deprotection and ester hydrolysis was performed by using a 33% solution of HBr in AcOH to provide the amino acid, which was immediately converted into Boc-(*S*)-MeAba-Gly-OH (**16**) by use of Boc_2O. This enantiomerically enriched building block was introduced into the dermorphin peptide sequence as described for the racemate. After cleavage from the resin, the first eluting epimer **7** was identified to contain (*S*)-α-MeAba, and hence the second eluting peptide was the corresponding *R* epimer, **8**.

Biological evaluation

The affinity and potency of compounds **1** and **5**–**8** for the μ- and δ-opioid receptors were determined by competition binding experiments of the ligands with the receptor selective radioligands [^{3}H]DAMGO (μ) and [^{3}H][Ile 5,6]deltorphin-2 (δ) in rat brain membrane homogenates (Table 2). Comparative analysis of the binding results revealed that (*S* or *R*)-α-MeAba 3- and (*S* or *R*)-Aba 3- modifications on the dermorphin structure, in general, yielded analogues that retained μ-receptor preferences and decreased receptor selectivities. The native ligand (**1**) showed affinity values consistent with the literature data,[52] and exhibited a far higher selectivity than those of analogues **5** to **8**. Among the analogues, two compounds (**5** and **8**) proved to be as potent as the parent dermorphin (**1**) on the basis of binding results; this suggests that they are more likely to adopt conformations suitable for high-affinity ligand binding than compounds **6** and **7**. Compared to the native dermorphin **1**, [(*S*)-Aba 3-Gly 4]dermorphin (**5**) maintained subnanomolar affinity for the μ-opioid receptor, but showed a tenfold increase in δ affinity. This is in agreement with our previous results.[18] The *R* epimer **6** was substantially less potent, although it still possessed low nanomolar affinity for the μ-receptor. Surprisingly, the [(*R*)-α-MeAba 3-Gly 4]dermorphin epimer (**8**) was much more potent than the *S* epimer, **7**. Compound **8** is about four-times less potent with the μ- and δ-receptors relative to the most potent ligand [(*S*)-Aba 3-Gly 4]dermorphin (**5**). Taking these findings together, it should be noted that the introduction of the methyl substituent at the α-position of Aba is, in the case of compound **8**, well tolerated by both opioid receptors.

Functional properties of the new ligands were assessed by the widely used ligand-stimulated [^{35}S]GTPγS binding assay. With regard to functionality, each ligand stimulated [^{35}S]GTPγS binding over the basal activity. The resulting values clearly indi-

Table 2. Receptor binding affinities and selectivities.

Peptide	[^{3}H]DAMGO K_i^{μ} [nM]	[^{3}H][Ile 5,6]deltorphin-2 K_i^{δ} [nM]	Selectivity K_i^{δ}/K_i^{μ}	EC_{50} [nM]	E_{max} [%]
Dermorphin (**1**)	0.2 ± 0.05	381 ± 31	1905	46 ± 2	155 ± 2
H-Tyr-D-Ala-[(*S*)-Aba-Gly]-Tyr-Pro-Ser-NH_2 (**5**)	0.3 ± 0.04	33. 3 ± 2.2	111	42 ± 7	175 ± 6
H-Tyr-D-Ala-[(*R*)-Aba-Gly]-Tyr-Pro-Ser-NH_2 (**6**)	10.3 ± 0.9	612 ± 18	59	855 ± 151	149 ± 2
H-Tyr-D-Ala-[(*S*)-α-MeAba-Gly]-Tyr-Pro-Ser-NH_2 (**7**)	252 ± 40	> 10000	–	2436 ± 397	123 ± 4
H-Tyr-D-Ala-[(*R*)-α-MeAba-Gly]-Tyr-Pro-Ser-NH_2 (**8**)	1.1 ± 0.1	134 ± 10	121	184 ± 35	153 ± 3

Receptor binding affinities and selectivities of native dermorphin (**1**) and its constrained heptapeptide analogues **5**–**8**, and their efficacies determined by the ligand-stimulated GTPγS functional assays. Data are means ± SEM of 3–5 independent experiments. No selectivity was determined when the K_i value proved to be higher than 10000.

cate that the ligands bind the opioid receptors and activate G proteins (Table 2). These data were compared to those of the prototypic μ-receptor ligand DAMGO ($EC_{50}=122$ nM, $E_{max}=178$%). As can be seen, each ligand showed an agonist character providing E_{max} values of 123 up to 175. Interestingly, the tendency of ligand potencies and efficacies correlated well with those of the K_i values, that is, ligands that had low or high μ-receptor affinities, displayed similarly low or high EC_{50} and proportional E_{max} values, suggesting profiles ranging from partial to full agonists. Considering these facts, it can be concluded that (*S* or *R*)-α-MeAba 3- or (*S* or *R*)-Aba 3- modifications of the heptapeptide dermorphin do not influence functionality and the ligands retain their G-protein binding and activating properties.

Conformational analysis of 5 to 8

Our previous studies on dipeptide amides containing Aba-Gly and α-MeAba-Gly demonstrated that the former adopted mainly extended structures and the latter showed a well-defined β turn.[21] To investigate the persistence of these features in the novel dermorphin compounds **5** to **8**, conformational studies by using NMR-based molecular modeling techniques were performed.

From the initial analysis of the 1D proton spectrum two distinct sets of signals were found to occur for each of the compounds. The population of the major set in **5** to **8** was determined at 82–86%. The presence in each compound of clear exchange correlation cross-peaks in 2D ROESY that connect both sets of resonances, indicates the presence of two conformations in slow exchange ($k_{ex}\sim 1\ s^{-1}$) on the NMR timescale. Their presence results from *cis–trans* isomerization of the Tyr 5-Pro 6 amide bond as proven by NOE contacts correlating Tyr 5 H_α with either the H_δ (major), or the H_α (minor; Figure S1, see the Supporting Information).

Assignments and conformational studies of **5**–**8** were restricted to the major conformation due to the low signal intensities of the minor conformation and were obtained from the analysis of 2D $^1H,^1H$ TOCSY and $^1H,^{13}C$ HSQC/HMBC 2D NMR spectra (Tables S3–S6 in the Supporting Information). Additional conformational dependent NMR spectroscopy parameters, that is, $^3J_{H\alpha HN}$ scalar couplings, H_N temperature coefficients and H_N hydrogen deuterium exchange rates (Table 3) were determined as described in the Experimental Section.

Hydrogen–hydrogen distances were extracted from 200 ms off-resonance ROESY spectra. The 47 interproton distances, consisting of 22 intraresidue and 25 inter-residue (i, $i+1$) were derived for **5**. For **6**, 62 proton–proton distance restraints were obtained including 31 inter-residue (i, $i+1$) contacts. Importantly, no long-range (i, $i+n$; $n>1$) contacts were observed for both **5** and **6**; this indicates that these molecules most likely adopt an extended structure, as expected. For **7**, 52 distance restraints were extracted corresponding to 25 intraresidue and 27 inter-residue NOE contacts including eight long-range contacts. These involve Ala 2 H_β, for which contacts to Tyr 5 H_N, H_β, H_δ and Ser 7 H_N, H_α, H_β were found. Additionally, contacts from Ala 2 H_N to Tyr 5 H_N and H_β were observed. Finally, 46 NOE contacts were assigned for **8**, consisting of 21 intraresidue, 21 inter-residue (i, $i+1$) and four long-range contacts. Two of these correlate with the Tyr 5 H_β protons with Ala 2 H_N and Ser 7 H_N. Furthermore, contacts from Ala 2 H_β to Tyr 5 H_δ and from Aba 3 H_ι (Figure S2, Supporting Information) to Pro 6 H_δ were present. From these observations, both **7** and **8** are expected to adopt a turn-like feature. The complete set of restraints used for all molecules is presented in Table S8 in the Supporting Information.

The results from this qualitative analysis of the data were validated by using NMR-based molecular modeling. Initially, a simulated annealing (SA) restrained MD protocol was used for **5** and **8**. However, analysis of the conformations sampled by SA for **5** revealed that on average 21 distance restraints (45%) were violated with maximum violations between 0.23 and 0.45 Å. The simulation reveals an extended N-terminal conformation with its C terminus folding back over the Aba 3 residue. The fact that the simulated annealing protocol does not generate any conformations that satisfy the majority of the NOE restraints at the same time, suggests some degree of conformational flexibility of **5**. Indeed, it is well known that flexible linear peptides that are able to adopt many low-energy conformations in solution, lead to averaging of the various NMR constraints. By imposing these averaged constraints, an averaged, virtual, and therefore, nonexistent conformation is generated, which does not represent the actual conformational space available to the peptide.

In order to address this, time averaged MD simulations (tar-MD)[53] were performed instead on compounds **5**–**8**. Such simulations generate a conformational ensemble that represents the conformational space, that is, on average over time, in

Table 3. Temperature coefficients and deuterium exchange rates of **5**–**8**.

	$\Delta\delta/\Delta T$ [ppb K^{-1}]		$t_{1/2}$ (D-exchange)		$^3J_{H\alpha HN}$ [Hz]			$\Delta\delta/\Delta T$ [ppb K^{-1}]		$t_{1/2}$ (D-exchange)		$^3J_{H\alpha HN}$ [Hz]	
	5	**6**	**5**	**6**	**5**	**6**		**7**	**8**	**7**	**8**	**7**	**8**
Tyr 1	−1.47	−1.60	1	1	5.64	5.16	Tyr 1	−1.40	–[a]	1	–[a]	5.75	–[a]
D-Ala 2	−4.47	−3.94	92	1	8.04	7.79	D-Ala 2	−4.07	−3.00	190	1	7.76	7.72
Aba 3	−6.10	−5.86	100	100	7.65	7.02	Aba 3	−5.50	−6.01	100	100	–[b]	–[b]
Tyr 5	−6.53	−6.48	58	100	8.22	8.32	Tyr 5	−5.03	−4.73	87	4000	8.43	8.22
Ser 7	−4.23	−4.29	17	29	7.85	8.86	Ser 7	−4.40	−5.03	33	400	7.97	7.96

Temperature coefficients in the 298 to 328 K interval, deuterium exchange half-lifetimes (normalized to Aba 3) and scalar coupling constants of amide protons (and ammonium protons for Tyr 1). [a] Ammonium protons not observed; [b] C_α-methylated residue.

agreement with the available NMR data. Therefore, NMR constraints need not be instantaneously and simultaneously satisfied and individually sampled conformations are allowed to violate part of the NMR data at any specific time point in the trajectory. Yet, this protocol forces each restraint to be satisfied on average over a certain simulation time interval (here chosen to be 8 ns).

A view of the conformational space sampled during the tar-MD trajectories for **5**–**8** is shown in Figure 2, and the distribution of main chain Φ,Ψ dihedral angles for the five internal residues are presented by using Ramachandran plots (Figure 3). These charts allow a better appreciation of the extent of the conformational space sampled by each individual amino acid backbone during the trajectory. Comparison with the Φ,Ψ dihedral angles obtained from the simulated annealing restrained MD protocol (Figure 3) clearly shows the detrimental impact of imposing averaged constraints, thereby generating virtual conformations with unfavorable energies. For **5**, for instance, the simulated annealing protocol results in a single Pro 6 population in an unfavorable area of the Ramachandran map, whereas application of tar-MD populates the two energetically favored conformations. For other residues, the local conformations, generated by the SA approach, fit quite well to the conformational space in the tar-MD ensemble (e.g., Aba 3).

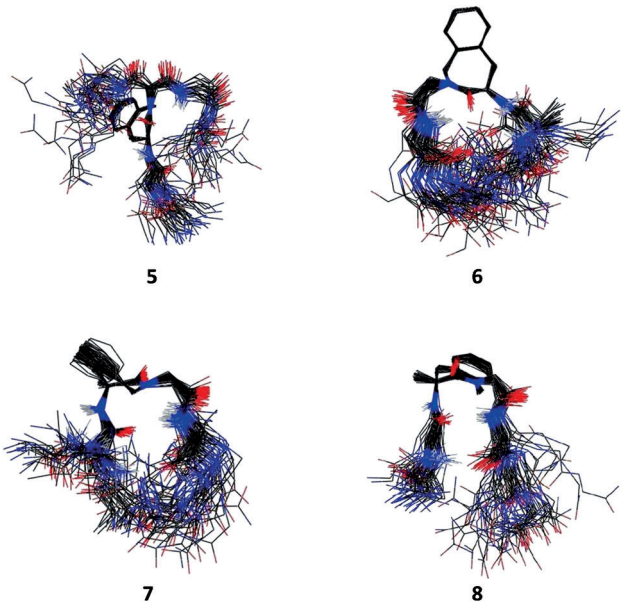

Figure 2. Overlay of 70 conformations of **5**–**8** uniformly sampled from the last 78 ns of 80 ns time-averaged restrained MD simulations. Superpositions are based on all heavy atoms of Aba 3 and Gly 4 residues. No side chains are shown except for Aba 3.

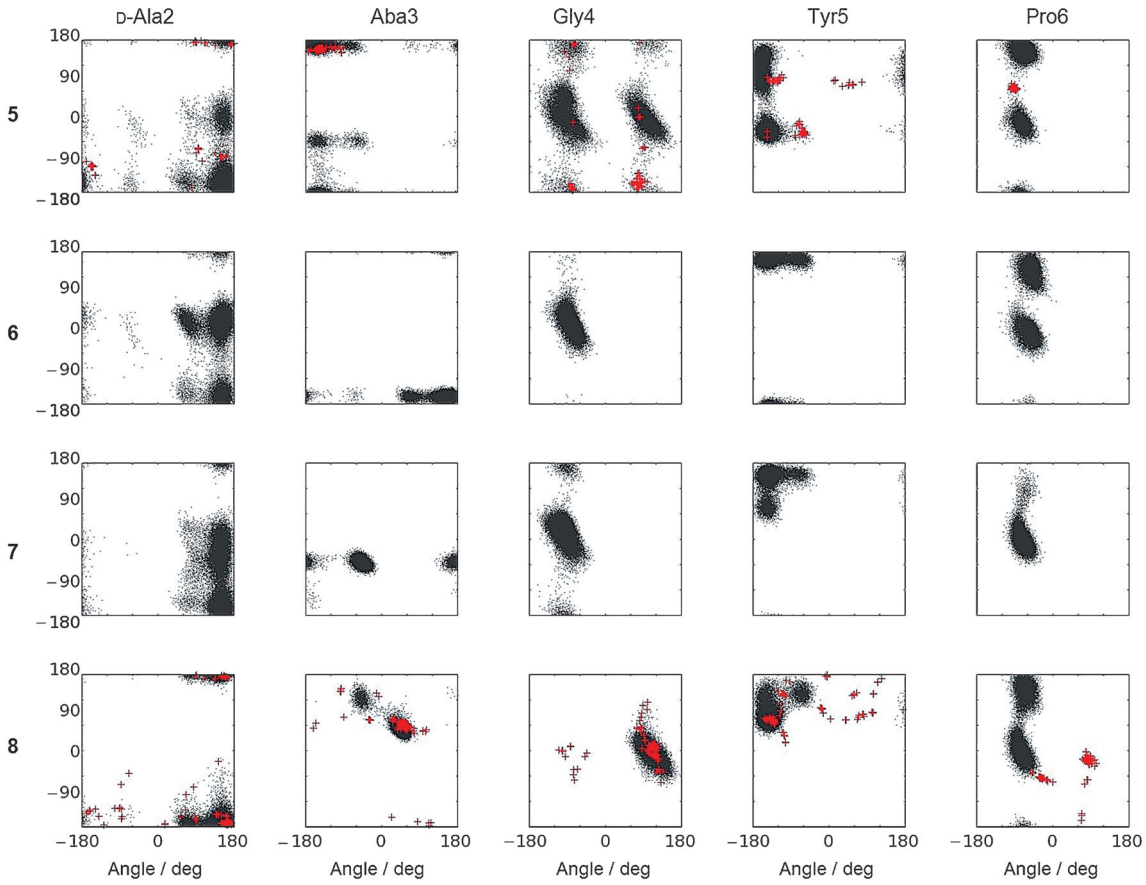

Figure 3. Ramachandran plots of dermorphin analogues **5** to **8** resulting from tar-MD (gray) and SA (red) simulations.

The most evident and unambiguous difference in conformation between the compounds that can be observed when comparing these plots is evident for the Aba 3 residue. Comparing **5**, **6** with **7**, **8** clearly shows the former pair to adopt mainly (and **6** exclusively) an extended conformation in the ensemble, whereas the latter pair adopt mostly (and **7** exclusively) a helical conformation, in agreement with the qualitative analysis above. The C-terminal Pro 6 is shown to cover the entire energetically allowed Φ,Ψ space, indicating flexibility at the C terminus. For **7**, however, the Ψ angle remains confined to the helical area. Within each group, the impact of the change in stereochemistry of the Aba 3 residue results mostly in the inversion of the populated areas, as can be expected. Similar conformational spaces are covered by D-Ala 2, with both extended and helical character present, except for **8**, in which only extended conformations appear (Figure 3). Other trends that can be observed are less general. While Tyr 5 populates clearly different areas when comparing **5** and **6**, which suggests a link to the Aba 3 stereochemistry, no such difference is apparent in **7** and **8**. Finally, the behavior of the Gly 4 residue is least amenable to interpretation. For **6**–**8**, mostly a single helical region is populated for this residue, but no evident link with the stereochemistry of the preceding Aba 3 is apparent.

While in **5**, the D-Ala 2-Aba 3 dipeptide is rather well-defined and mostly occupies an extended conformation, the larger Φ,Ψ space accessed by the Gly 4-Tyr 5 dipeptide in **5** suggests a more flexible C-terminal segment, whereby the C terminus is folded back towards the N terminus by two distinct conformations on opposing sides of the molecule, as clearly evident from Figure 2. Despite this back-folding, no turn-like structure is adopted. Furthermore, no hydrogen bonds were observed in this set of molecules, which is in good agreement with the measured temperature coefficients and hydrogen–deuterium exchange rates.

Considering that on average 19 distance restraints (40%) were still violated with a maximum violation of 0.35 Å in the tar-MD trajectory of **5**, no significant drop in violations is observed when compared to the previous simulated annealing results. In all, **5** can be considered a flexible molecule without any regular structural elements.

On average, 13 distance restraints (21%) were violated for **6** with an average violation of 0.11 Å, giving a satisfactory agreement. Here, the backbone of Gly 4 and Tyr 5 is restricted to one single conformation. Compared to **5**, this results in a peptide conformation in which the C terminus is still folded toward the N terminus of the peptide but only along one side of the Aba 3 residue, resulting in a more defined overall conformation. Again, no stabilizing hydrogen bonds were observed in the set of conformations modeled and no classical turn-like structure is adopted. This agrees with the experimental temperature coefficients and hydrogen–deuterium exchange rates measured. In all, the core tripeptide of **6** can be considered to adopt a single but rather flexible conformation without any regular structural elements.

For **8**, 19 distance restraints were violated on average, but none more than 0.37 Å while the measured $^3J_{HNH\alpha}$ scalar coupling constants of D-Ala 2 and Ser 7 were reproduced within 0.4 and 0.2 Hz, respectively. For the Tyr 5 residue a scalar coupling of 7.3 Hz was obtained during the tar-MD simulation (experimental: 8.22 Hz). This simulation clearly shows well-defined major and minor conformations for the D-Ala 2, Aba 3, Gly 5 residues and a single conformation for Gly 5, while Pro 6 populates two conformations similar to those observed for **5** and **6**. Overall, a clear turn structure is visible over Aba 2-Gly 3, which is closed by a hydrogen bond involving Tyr 5 H_N and D-Ala 2 CO. In the major conformation, a second hydrogen bond is additionally present between D-Ala 2 H_N and Tyr 5 CO. For the minor conformation the C-terminal residues adopt a wider range of conformations. The distance and angles defining the geometry of the Tyr 5 H_N to D-Ala 2 CO hydrogen bond is presented in Figure 4, which shows that values leading to an energetically favorable geometry (i.e., 2.4 Å and 150° for the hydrogen bond distance and angle, respectively) is on average adopted in the ensemble.

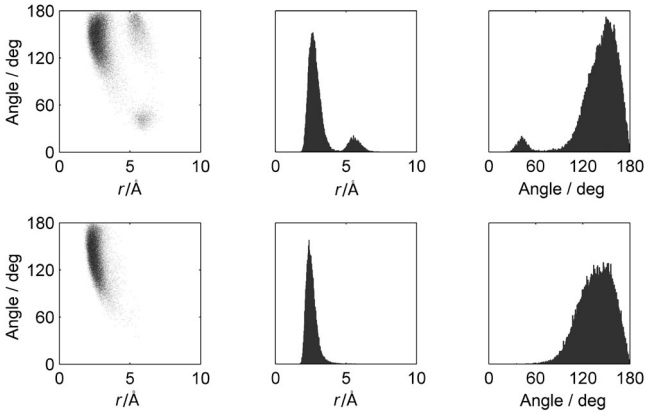

Figure 4. N–H↔O=C distances (Å) and angles (°) of the D-Ala 2 H_N···Tyr 5 CO hydrogen bond observed during tar-MD simulations of **7** (top panel) and **8** (lower panel).

For the second hydrogen bond, values of 2.6 Å and 120° were obtained, indicating a less optimal geometry. Based on the mean ϕ and ψ angles of Aba 3 (47°, 55°) and Gly 4 (118°, −10°), this turn structure can be classified as a type I′ β-turn. The stability of the secondary structure element is supported by the very slow exchange rate of Tyr 5 H_N, which also features a lower temperature coefficient of $-4.73\ ppb\,K^{-1}$ (cfr. $-6.48\ ppb\,K^{-1}$ for **6**). An even smaller temperature dependence of $-3.00\ ppb\,K^{-1}$ is observed for the D-Ala 2 residue. However, the D-Ala 2 H_N can be efficiently exchanged. This is in line with the fact that this hydrogen bond is not persistent since it is not featured in the minor conformation.

Finally, the most populated conformation of the Aba 3 and Gly 4 residues in **7** presents an inverse geometry with respect to **8** (Figure 3). This is further reflected in the seven-membered ring geometry (Table 4).

A turn-like structure is again apparent, closed by the same Tyr 5 H_N to D-Ala 2 CO hydrogen bond as in **8**. Given the inversion of all torsion angles of the Aba 3-Gly 4 dipeptide, com-

Table 4. Aba3 conformation of **5**–**8**.

	%	Aba3 φ	Aba3 ψ	Aba3 $\chi1$	Aba3 $\chi2$	Aba3 $\chi5$	Aba3 $\chi4$
5	94.1	−165	175	180	0	−60	60
6	100	165	−165	180	0	50	−65
7	100	−50	−50	60±20	15±20	50	−60
8	92.8	60	60	−65±20	−5±20	−45	55

Population (%) and geometry (dihedral angles, deg, see Figure 1) of the major conformation of the seven-membered ring in four dermorphin analogues **5**–**8** from the 80 ns tar-MD simulations.

pared to **7**, this turn can be classified as a type I β turn. The hydrogen bond has a similar and favorable geometry as the corresponding one in **8** (Figure 3), but is less persistent during the simulation, since it is clearly absent during a short time in the tar-MD trajectory. The existence of a second hydrogen bridge involving D-Ala2 H_N was only observed during about 20% of the total simulation. The existence of the hydrogen bond involving Tyr5 H_N and D-Ala2 CO is corroborated by the many long-range NOE contacts observed in this compound. On the other hand, the measured temperature dependence of the amide protons and their hydrogen–deuterium exchange rates are not clearly indicative for this feature as a considerably fast deuterium exchange rate was recorded for Tyr5 H_N in **7**, supporting a lower persistence than in **8**. Even though the latter experimental parameters average over a much longer time scale than the one sampled during the simulation, the combined result does suggest a more stable β-turn closing hydrogen bond in **8** than in **7**.

In none of the analogues **5**–**8**, evidence for a stacking of the D-Ala2 methyl between the Tyr1 and Aba3 aromatic rings, as found for the parent dermorphin (**1**), was observed. The chemical shift of the D-Ala2 methyl signals was found at 1.11 to 1.13 ppm and not below 1 ppm as for **1**. Remarkably, the ring conformation of the seven-membered azepinone ring of Aba3 is different in the non-α-methylated analogues **5** and **6**, in which the χ_1 is *trans*, compared to the α-methylated analogues **7** and **8**, in which χ_1 is *gauche* (Table 3). In contrast, previous conformational studies on Ac-α-MeAba-Gly-NH-Me have shown a *trans* ring conformation in solution and in the crystal.[21] Theoretical conformational studies showed that the *gauche* conformation was the lowest energy one, the *trans* having 2.34 kJ mol^{-1} higher energy. This indicates that the peptide sequence is able to switch preference between the two conformations.

Conclusions

Asymmetric phase-transfer catalysis was not able to provide (*S*)-α-Me-*o*-cyanophenylalanine (**12**) in acceptable enantiomeric purity. However, by using a Schöllkopf chiral auxiliary, this important intermediate was obtained in 88% *ee*, and it was further transformed into (*S*)-α-MeAba-Gly (**16**). This allowed the preparation of the Phe3 constrained analogues of dermorphin **7** and **8**, and to compare the opioid affinities, selectivities and functional properties to those of the non-α-methylated Aba-dermorphin analogues **5** and **6**. In agreement with previous results, the [(*S*)-Aba3-Gly4]dermorphin (**5**) retained μ-opioid affinity but displayed an increased δ affinity. The corresponding *R* epimer **6** was much less potent. In contrast the [(*R*)-α-MeAba3-Gly4]dermorphin isomer **8** was more potent than its *S* epimer, **7**. This is in agreement with previous results for the related [spiro-Aba3-Gly4]endomorphin isomers, for which the *R* epimer is the most potent, whereas in [Aba3-Gly4]endomorphin the *S* enantiomer is the most potent.[54]

For the non-methylated dermorphin analogues **5** and **6**, tar-MD simulations showed a degree of folding of the C terminus residues toward the N terminus of the peptide, without adopting a stabilizing β-turn conformation, however, and with considerable flexibility, especially for **5**. Both **7** and **8**, on the other hand, exhibited a type I/I′ β-turn conformation over the Aba3 and Gly4 residues stabilized by a hydrogen bond involving Tyr5 H_N and D-Ala2 CO. For **8** this is nicely correlated to the hydrogen–deuterium exchange rate. For **7** the modeling results indicate that this hydrogen bond is less persistent and is therefore not reflected in its hydrogen–deuterium exchange rate. A second hydrogen bond involving D-Ala2 H_N and Tyr5 CO has been observed in **8**, although also in this case its persistence is not clearly reflected in its hydrogen–deuterium exchange rate. This conformational study clearly shows the influence of the methylation of Aba3 C_α on the conformational behavior of these dermorphin analogues in [D_6]DMSO solution. However, the Aba3 C_α stereochemistry has been shown to have less effect on the overall conformational preference of the peptide.

The opioid receptor affinities of analogues **5** and **8** were shown to be very similar. Nevertheless, both analogues show a different conformational preference. This might indicate that these flexible ligands are able to adapt their conformation on binding to the receptor in order to obtain a common binding topography of the pharmacophoric groups.

Experimental Section

General: All Boc-protected amino acids-AA-OH were obtained from Fluka (Bornem, Belgium) as well as diisopropylcarbodiimide (DIC), 1-hydroxybenzotriazole (HOBt), trifluoroacetic acid (TFA), and dichloromethane. The MBHA resin (0.95 mmol g^{-1}) was purchased from Neosystem (Strasbourg, France). All other reagents were from Sigma–Aldrich (Bornem, Belgium). 2-1*H*(Benzotriazol-1-yl)-1,1,3,3-tetramethyluronium tetrafluoroborate (TBTU) was purchased from Senn Chemicals (Dielsdorf, Switzerland). H-Tyr-D-Ala-NMePhe-Gly-ol (DAMGO), tris(hydroxymethyl)aminomethane (Tris, free base), bovin serum albumin (BSA), guanosine-5′-[γ-thio]triphoshate (GTPγS), inorganic salts, organic solvents and HCl (37%) were purchased from Sigma–Aldrich and Molar, Kft. (Budapest, Hungary). The tritiated opioid ligands were prepared in the Isotope Laboratory of the Biological Research Center (HAS-BRC, Hungary). The radiolabeled GTPγS ([^{35}S]GTPγS; specific activity ≥1000 Ci mmol^{-1}) was ordered from the Izotop Intezet, Kft. (Hungary).

RP-HPLC (Waters Breeze analytical HPLC system) was performed by using a RP C-18 column (Supelco Discovery BIO Wide Pore C-18, l=25 cm, d=0.45 cm, PS=5 μm) with a mobile phase consisting of water/acetonitrile containing TFA (0.1%). Products were eluted

by using the gradient: $t=0$ min, 3% CH_3CN, $t=20$ min, 97% CH_3CN; flow-rate: 1.0 mL min^{-1}, $\lambda=215$ nm. Preparative HPLC (Gilson semipreparative HPLC system) was performed by using a RP C-18 column (Supelco Discovery BIO Wide Pore C-18, $l=25$ cm, $d=2.12$ cm, $PS=10$ μm) with the above-mentioned gradient at a flow-rate of 20.0 mL min^{-1}. TLC analysis was performed on plastic sheets precoated with silica gel 60F_{254} (Merck). Melting points were measured with a Büchi B 540 melting point apparatus, with a temperature increment of 1 °C min^{-1}. ^{1}H and ^{13}C NMR spectra were recorded at 250.13 and 62.90 MHz, respectively, with a Bruker Avance DRX250 spectrometer, by using TMS or the residual solvent signal as internal reference. Mass spectra were recorded on a VG Quattro^{II} spectrometer by using electrospray ionization in positive ion mode (Micromass, Manchester, UK). For LCMS recording, a Waters Breeze analytical HPLC with manual injector, UV detector (2487, 215 nm) and Waters 600E pump was coupled to the VG Quattro^{II} spectrometer. The runs were performed on a reversed phase C-18 column (Supelco Discovery BIO Wide Pore C-18, $l=25$ cm, $d=4.6$ mm, $PS=5$ μm) with a mobile phase consisting of water/acetonitrile containing TFA (0.1%). Products were eluted by using the gradient: $t=0$ min, 3% CH_3CN, $t=20$ min, 97% CH_3CN; flow-rate: 1.0 mL min^{-1}, $\lambda=215$ nm.

Peptide synthesis

Peptide synthesis was performed manually in fritted polypropylene syringes (10 mL), which were shaken during coupling, washing, deprotection and cleavage steps. The N-terminal dermorphin analogues **1** and **5**–**8** were manually prepared by solid-phase synthesis by using Boc chemistry and the MBHA resin (0.95 mmol g^{-1}) as solid support. The resin was swollen in CH_2Cl_2 for 1 h followed by treatment with 20% DIPEA/CH_2Cl_2 to neutralize. Side chain protecting groups were used in the case of Ser(Bn) and Tyr(2,6-Cl_2Bn). Peptides **5** and **6** were prepared by using a threefold excess of the amino acids and a twofold excess of the (*S*)-Aba-Gly and (*R*)-Aba-Gly building blocks together with TBTU (4 and 3 equiv, respectively) as a coupling reagent and DIPEA (8 and 6 equiv, respectively) as base in a mixture of anhydrous DMF/anhydrous CH_2Cl_2 (1:1). A threefold excess of the amino acids and coupling reagent (DIC) were used together with a threefold excess of HOBt anhydrous in a DMF/anhydrous CH_2Cl_2 (1:1) solvent mixture to prepare peptides **7** and **8**. The completeness of the couplings was checked with the NF-31 test.[55] If incomplete, the coupling was repeated. Boc deprotections were performed in 50% TFA/2% anisol/CH_2Cl_2 (1×10 and 1×20 min). When the SPPS was completed, the resin was washed with CH_2Cl_2 three times and then neutralized with 20% DIPEA/CH_2Cl_2 solution (3×1 min). Between every coupling, deprotection and cleavage step the resin was washed three times with DMF, *i*PrOH and CH_2Cl_2. Final cleavage of the peptide from the resin was done by treatment with HF_{liq} (Asti, France) for 1 h at 0 °C. Anisol (2 mL) and HF_{liq} (10 mL) were used for 1 g peptide–resin. After evaporation of the HF under vacuum the crude peptide was precipitated with cold dry ether and filtered. The precipitated peptide and resin beads were washed with glacial acetic acid. The filtrate was lyophilized and these crude mixtures were purified by preparative HPLC with a final purity >99%. Peptide purity and identity was determined by LCMS.

Biology

Radioligand binding assay: For competitive binding experiments, rat brain membrane homogenate (Wistar, male, 250–300 g body weight) was prepared as described elsewhere.[56] Animals were treated according to the European Communities Council Directives (86/609/ECC) and the Hungarian Act for the Protection of Animals in Research (XXVIII.tv. 32.§). The protein content of the homogenate was determined by the method of Bradford[57] by using BSA as standard. The protein concentration ranged between 0.2–0.4 mg per test tube. The following conditions were applied to assess inhibitory constants: [^{3}H]DAMGO (25 °C, 1 h, GF/C filter, glass tube), [^{3}H][Ile 5,6]deltorphin-2 (35 °C, 45 min, GF/B filter, plastic tube, 0.25 mg BSA per tube). The incubation mixtures were filled to a final volume of 1 mL with Tris-HCl buffer (50 mM, pH 7.4) and samples were incubated in a shaking water-bath at the appropriate temperature. Competition binding experiments were performed by incubating the membranes with [^{3}H]DAMGO (0.5 nM), [^{3}H][Ile 5,6]deltorphin-2 (2 nM) and increasing concentrations (10^{-11}–10^{-5} M) of the unlabeled dermorphin analogues. Nonspecific binding was determined with naloxone (10 μM) and subtracted from the total binding to yield specific binding. Incubation was initiated by the addition of the membrane suspension and stopped by rapid filtration over Whatman GF/C or GF/B glass fiber filters, by using a Brandel cell harvester. Filters were washed with ice-cold Tris-HCl buffer (pH 7.4; 3×5 mL), and then the filter-bound radioactivity was measured in an Optiphase Supermix scintillation cocktail (PerkinElmer) by using a TRI-CARB 2100TR liquid scintillation counter. Each experiment was performed in duplicate and analyzed by the one/two-site binding competition fitting option of the GraphPad Prism software (Version 4).

Ligand-stimulated [^{35}S]GTPγS functional assay: Ligand-stimulated [^{35}S]GTPγS binding was performed as described elsewhere.[58] Briefly, rat brain membranes (15 μg protein per tube) were incubated with [^{35}S]GTPγS (0.05 nM) and opioids (10^{-10}–10^{-5} M) in the presence of GDP (30 μM), NaCl (100 mM), $MgCl_2$ (3 mM) and EGTA (1 mM) in Tris-HCl buffer (50 mM, pH 7.4) for 60 min at 30 °C. Basal binding activity was measured in the absence of opioids and was corrected with the nonspecific binding to yield specific binding. Nonspecific binding was determined with unlabeled GTPγS (10 μM). The reaction was initiated by the addition of the protein and terminated by the addition of ice-cold buffer (5 mL, 50 mM Tris-HCl, pH 7.4); then the samples were filtered through a Whatman GF/B glass fiber filter by using a Brandel cell harvester. Vials were washed three times with ice-cold buffer (5 mL), and then immersed in Optiphase Supermix scintillation cocktail. The radioactivity was measured by using a TRI-CARB 2100TR liquid scintillation counter. Ligand stimulations were expressed as a percentage of the specific [^{35}S]GTPγS binding over the basal activity. Each measurement was performed in triplicate and analyzed by the sigmoid dose-response curve fitting option of the GraphPad Prism software (Version 4).

NMR investigation of 5–8

Samples are prepared by using standard high performance 5 mm NMR spectroscopy tubes with solutions of **5**–**8** (~5 mM) in [D_6]DMSO. All experiments used for assignments were performed either on a Bruker DRX spectrometer (**5**, **8**) equipped with a 5 mm TXI-Z probe and operating at a ^{1}H and ^{13}C frequency of 500.13 and 125.77 MHz, respectively, or on a Bruker Avance^{II} spectrometer (**6**, **7**) equipped with a 5 mm TXI-Z probe and operating at a ^{1}H and ^{13}C frequency of 700.13 and 176.06 MHz, respectively. The temperature used was 298 K throughout. All 1D and 2D experiments were performed by using pulse sequences available from the standard Bruker library.[59] Gradient enhanced sequences were used for the COSY and heteronuclear 2D experiments. TOCSY mixing times of 200 ms range were used. The HMBC spectra were optimized for

8 Hz long-range $^{n}J_{CH}$ couplings. Typically, 2D spectra consisted of 512 t_1 increments of 8–32 scans each, sampled with 4 k points. Prior to Fourier transformation, the data were zero-filled along t_1 and suitably apodized by using a squared cosine bell in both dimensions, except for the COSY and HMBC, for which a squared sine bell was used. The ^{1}H chemical shifts were obtained by using 1D proton NMR spectroscopy if resolved or deduced from 2D NMR cross-peaks otherwise.

Temperature coefficients were measured from additional 1D proton NMR spectra at 308, 318 and 328 K. The $^3J_{HH}$ scalar coupling constants were extracted from the 1D ^{1}H spectrum at 298 K. The ^{1}H–^{2}H exchange rates of amide protons were obtained by integrating amide resonances from 1D ^{1}H spectra recorded after spiking the sample with a small amount of D_2O. All processing and analysis of these spectra was performed by using Bruker TopSpin 2.1 software suite.

NMR distance restraints for **5**–**8** were extracted from ^{1}H–^{1}H off-resonance ROESY spectra[60] recorded at a magnetic field strength of 700.13 MHz for protons. The 4 k by 1 k data points were recorded in the direct and indirect dimension, respectively. Then 64 scans were recorded for each increment by using a total interscan relaxation delay of 1.9 s. Off-resonance irradiation was performed during 200 ms by using a irradiation strength of 10 kHz and an offset of ±5773.5 Hz. Spectra were Fourier transformed after apodization with squared cosine window functions in both dimensions resulting in a spectrum of 4 k by 4 k data points.

Cross-peaks were assigned and integrated manually within the CC NMR software suite[61] and converted to interproton distances by using an R^{-6} conversion. Contacts between methylene moieties were used as a calibration for this conversion. Upper boundaries were set at 110% of the experimental NOE distance while lower boundaries were fixed at 1.8 Å. Non-stereospecific NOE contacts were treated by introducing pseudoatoms and increasing the upper bound of the restraint by a fixed value.[62]

Molecular modeling of 5–8

Molecular modeling studies by using the classical simulated annealing[63,64] approach were performed within the Discover3 module of Insight^{II} (Accelrys) by using the built-in consistent force field (CFF91).[53] Partial atomic charges were generated by using the standard module within InsightII. A distance dependant scaling for electrostatic interactions was used as a basic implicit solvent model in all calculations. During an initial unrestrained MD simulation of 5.5 ns at 1000 K, 100 conformations of **5** to **8** were uniformly sampled over the last 5 ns of the trajectory. While subjecting each of these 100 conformations to the experimental NOE distance constraints short MD (1.5 ps) simulations were subsequently ran at decreasing temperatures down to 300 K. At 300 K, an additional 4 ps MD simulation was performed. NOE distance restraints were introduced by using 40 kcal mol^{-1} Å^{-2} harmonic potentials when the experimental distance boundaries were exceeded. Additionally, each conformation obtained was subjected to a full restrained energy minimization by using the same potential for the NOE restraints. During all simulations, dihedral angle restraints were introduced by keeping each peptide bond in the *trans* configuration. No scalar couplings were used as restraints within the molecular modeling scheme.

Molecular modeling studies by using the time-averaged restraints molecular dynamics (Tar-MD) approach[65] were performed within the Sander module of AMBER9[66] with the built-in GAFF[67] force field. AM1-BCC charges[68] generated by the antechamber module were used as partial atomic charges for **5**–**8**. Averaging of restrained proton–proton distances was performed by using an R^{-6} relationship and an exponentially decaying function [Eq. (1)]. The memory decay constant, τ, was set to 8 ns. These restraints were used in a single 80 ns MD simulation at 300 K by using a scaling factor of 57 (corresponding to DMSO) for electrostatic interactions as basic implicit solvent model.

$$R_{TAR}(t)^{-6} = \frac{\int_0^t R(t')^{-6} e^{(t'-t)/\tau} dt'}{\int_0^t e^{(t'-t)/\tau} dt'} \quad (1)$$

NOE distance restraints were introduced by using 2 kcal mol^{-1} Å^{-2} flat-bottomed harmonic potentials. During all simulations, dihedral angle restraints were introduced by keeping each peptide bond in the *trans* configuration. No scalar couplings were used as restraints within the molecular modeling scheme.

Synthesis

2-(((2*R*,5*S*)-2-Isopropyl-3,6-dimethoxy-5-methyl-2,5-dihydropyrazin-5-yl)methyl)benzonitrile (18): A solution of *t*BuLi (1.6 M; 15.75 mL, 25.2 mmol) was added dropwise to a solution of (2*R*,5*SR*)-2-isopropyl-3,6-dimethoxy-5-methyl-2,5-dihydropyrazine (**17**; 5.0 g, 25.2 mmol, 5 mL, $\rho = 1$ g mL^{-1}) in dry THF (50 mL) under argon atmosphere at −78 °C. The resulting solution was stirred at −78 °C for 1 h and treated carefully with a solution of *o*-cyanobenzyl bromide (6.5 g, 33.3 mmol, 1.32 equiv) in dry THF (70 mL). The reaction mixture was stirred at −78 °C for 10 h. The mixture was allowed to warm slowly to room temperature and was subsequently quenched with a saturated NH_4Cl solution (80 mL). The aqueous layer was twice extracted with Et_2O (80 mL). The combined organic phases were washed with brine (150 mL) and dried over $MgSO_4$. After removal of the solvent in vacuo, the crude was purified by flash column chromatography (CH_2Cl_2/petroleum ether 1:1→100% CH_2Cl_2) to give **18** (5.7 g, 72%): $R_f = 0.40$ (CH_2Cl_2/$CHCl_3$ 9:1); mp: 51.2–53.9 °C; $[\alpha]_D = +15$ ($c = 1$ in CH_2Cl_2); ^{1}H NMR (DMSO, 250 MHz) $\delta_H = 0.51$ (d, $J = 6.8$ Hz, 3H), 0.89 (d, $J = 6.9$ Hz, 3H), 1.43 (s, 3H), 2.04 (m, 1H), 3.03 (d, $J = 13.1$ Hz, 1H), 3.17 + 3.24 (AB system, $J_{AB} = 13.1$ Hz, 2H), 3.63 (s, 6H), 7.17 (d, $J = 7.4$ Hz, 1H), 7.37 (t, $J = 7.6$ Hz, 1H), 7.56 (t, $J = 7.7$ Hz, 1H), 7.70 ppm (d, $J = 7.7$ Hz, 1H); ^{13}C NMR (DMSO, 63 MHz) $\delta_C = 16.2$, 19.1, 28.4, 29.9, 44.5, 52.0, 52.1, 59.1, 59.6, 113.4, 118.2, 127.4, 130.6, 132.4, 132.5, 140.3, 161.5, 163.1 ppm; MS (ES+): *m/z* 314 $[M+H]^+$, 282, 197; HPLC t_R = 19.9 min.

α-Methyl-(*S*)-*o*-cyanophenylalanine hydrochloride (12): Trifluoroacetic acid (10.3 mL) was added to a solution of 2-(((2*R*,5*S*)-2-isopropyl-3,6-dimethoxy-5-methyl-2,5-dihydropyrazin-5-yl)methyl)benzonitrile (**18**; 5.6 g, 17.9 mmol) in acetonitrile/water (82 mL, 3:1) and the resulting solution was stirred, overnight (~10 h). After evaporation, the residue was diluted with ethyl acetate (100 mL) and water (80 mL). The aqueous layer was neutralized with a 5% solution of $NaHCO_3$ and extracted with CH_2Cl_2 (4×80 mL). The organic phase was dried over $MgSO_4$ and evaporated to give α-methyl-(*S*)-*o*-cyanophenylalanine methyl ester hydrochloride (4.1 g, 100%); $R_f = 0.66$ (EBAW); mp: 59.8–62.4 °C; $[\alpha]_D = -3.8$ ($c = 1$ in CH_2Cl_2); ^{1}H NMR (DMSO, 250 MHz) $\delta_H = 0.83$ (br s, 2H), 1.19 (s, 3H), 3.04 (d, $J = 3.7$ Hz, 1H), 3.09 (d, $J = 5.4$ Hz, 1H), 3.63 (s, 3H), 7.39–7.46 (m, 2H), 7.61 (t, $J = 7.6$ Hz 1H), 7.75 ppm (d, $J = 7.7$ Hz, 1H); ^{13}C NMR (DMSO, 63 MHz) $\delta_C = 24.7$, 44.1, 51.9, 58.3, 113. 2, 118.40

(–CN), 127.4, 131.5, 132.4, 132.6, 140.5, 176.4 ppm; MS (ES+): *m/z* 437, 219 $[M+H]^+$, 159; HPLC t_R = 9.5 min.

Next, a solution of α-methyl-(*S*)-*o*-cyanophenylalanine methyl ester hydrochloride (3.9 g, 17.9 mmol, 1.0 equiv) in HCl (6 N, 70 mL) was stirred for 55 h at 65 °C and subsequently cooled to room temperature, which induced partial crystallization. The white crystals were filtered and rinsed with a minimum amount of cold HCl (6 N). The remaining product was obtained after evaporation under high pressure (2.8 g, 0.8 g crystals + 2.0 g crude; 65%): R_f = 0.51 (EBAW); mp: 192.8–194.1 °C; $[\alpha]_D$ = −5.0 (*c* = 1 in H_2O); ^{1}H NMR (DMSO, 250 MHz) δ_H = 1.46 (s, 3H), 3.34 (d, *J* = 14.2 Hz, 1H), 3.40 (d, *J* = 14.4 Hz, 1H), 7.48 (d, *J* = 7.4 Hz, 1H), 7.54 (t, *J* = 7.7 Hz, 1H), 7.68 (t, ^3J = 7.4 Hz, 1H), 7.82 (d, *J* = 7.6 Hz, 1H), 8.85 ppm (br s, 3H); ^{13}C NMR (DMSO, 63 MHz) δ_C = 20.7, 40.0, 59.1, 113.3, 117.8, 128.4, 131.8, 133.1, 137.4, 171.4 ppm; MS (ES+): *m/z* 205 $[M+H]^+$, 159; HPLC t_R = 8.3 min; *ee* (%) 88.

***N*-Methyloxycarbonyl-α-methyl-(*S*)-*o*-cyanophenylalanine (13)**: Methylchloroformate (8.7 mL, 113.0 mmol, 10.0 equiv) was added to a solution of α-methyl-(*S*)-*o*-cyanophenylalanine hydrochloride (**12**; 2.7 g, 11.3 mmol, 1.0 equiv) in a NaOH solution (1 N, 80 mL). After being stirred for 1 h, the reaction mixture was cooled by use of an ice-bath and acidified to pH 2–3 with HCl (6 N). The aqueous phase was extracted with cold CH_2Cl_2 (4×140 mL). The combined organic layers were washed with water (pH 2, 1×140 mL). The organic phase was dried ($MgSO_4$), filtered and evaporated. A yellow oil was obtained and used in the next step without further purification (2.1 g, 70%): R_f = 0.83 (EBAW); $[\alpha]_D$ = −17.6 (*c* = 1 in CH_2Cl_2); ^{1}H NMR (DMSO, 250 MHz) δ_H = 1.14 (s, 3H), 3.24 (d, *J* = 13.7 Hz, 1H), 3.49 (d, *J* = 14.3 Hz, 1H), 3.56 (s, 3H), 7.27 (d, *J* = 7.7 Hz, 1H), 7.44 (t, *J* = 7.6 Hz, 1H), 7.64 (t, *J* = 7.6 Hz, 1H), 7.78 ppm (d, *J* = 7.7 Hz, 1H); ^{13}C NMR (DMSO, 63 MHz) δ_C = 22.3, 38.5, 51.4, 58.7, 113.6, 118.4, 127.6, 132.0, 132.7, 132.9, 140.5, 155.6, 174.9 ppm; MS (ES+): *m/z* 809, 547, 285 $[M+Na]^+$, 217, 188; HPLC t_R = 11.8 min.

4-(*S*)-Methyloxycarbonylamino-4-methyl-1,2,4,5-tetrahydro-2-benzazepin-3-one (14): Pd/C (10%, 40 wt.%, 0.796 g) and an aqueous AcOH solution (10%, 5.9 mL, 11.4 mmol, 1.5 equiv) were added to a suspension of *N*-Moc-α-methyl-(*S*)-*o*-cyanophenylalanine (**13**; 2.0 g, 7.6 mmol, 1.0 equiv) in EtOH/H_2O (3:1, 65 mL). The suspension was hydrogenated in a Parr apparatus (0.34 mpa, room temperature, 2 days). The mixture was filtered over dicalite and rinsed with water. After evaporation of the solvent, the residue was crystallized from a minimum amount of hot EtOH and gave *N*-methyloxycarbonylamino-α-methyl-(*S*)-*o*-aminomethylphenylalanine (1.7 g, 85%): R_f = 0.69 (EBAW); mp: 219.2–220.1 °C; $[\alpha]_D$ = +2.4 (*c* = 1 in H_2O); ^{1}H NMR (DMSO, 250 MHz) δ_H = 1.52 (s, 3H), 3.01 (d, *J* = 13.8 Hz, 1H), 3.30 (d, *J* = 13.7 Hz, 1H), 3.57 (s, 3H), 3.80 (d, *J* = 13.0 Hz, 1H), 4.02 (d, *J* = 13.1 Hz, 1H), 6.65 (br s, 1H), 7.07 (d, *J* = 6.9 Hz, 1H), 7.16–7.27 (m, 3H), 8.45 ppm (br s, 2H); ^{13}C NMR (DMSO, 63 MHz) δ_C = 24.8, 36. 7, 40.1, 51.0, 60.5, 126.1, 128.1, 130.6, 131.3, 132.8, 138.4, 154.4, 175.1 ppm; MS (ES+): *m/z* 289, 267 $[M+H]^+$, 250, 204, 190; HPLC t_R = 8.1 min.

Next, a solution of *N*-Moc-α-methyl-(*S*)-*o*-aminomethylphenylalanine (1.64 g, 6.2 mmol, 1.0 equiv) and pyridine (1 mL, 12.4 mmol, 2.0 equiv) in CH_3CN/H_2O (3:1, 500 mL) was cooled in an ice-bath for 10 min, followed by the addition of *N*-(3-methylaminopropyl)-*N*′-ethylcarbodiimide (1.55 g, 8.1 mmol, 1.3 equiv, EDC). After 30 min the ice-bath was removed and the reaction mixture was stirred, overnight. After evaporation of the solvent, a white solid was obtained. This residue was redissolved in water (300 mL) and extracted with CH_2Cl_2 (4×300 mL). The organic layer was washed with H_2O (2×240 mL), dried ($MgSO_4$), filtered and evaporated. The combined aqueous phases were evaporated again, redissolved in H_2O (300 mL), and extracted with CH_2Cl_2 (3×300 mL). The organic layer was washed with H_2O (150 mL), dried ($MgSO_4$), filtered and evaporated to yield a white solid (1.3 g, 87%): R_f = 0.13 (EtOAc); mp: 187.2–188.6 °C; $[\alpha]_D$ = +31.7 (*c* = 1 in CH_2Cl_2); ^{1}H NMR (DMSO, 250 MHz) δ_H = 0.99 (s, 3H), 2.52 (d, *J* = 13.2 Hz, 1H), 3.53 (s, 3H), 3.79 (dd, *J* = 14.5, 7.7 Hz, 1H), 3.99 (d, *J* = 13.8 Hz, 1H), 4.58 (d, *J* = 14.3 Hz, 1H), 7.12–7.26 (m, 4H), 7.64 (s, 1H), 7.80 ppm (d, *J* = 6.1 Hz, 1H); ^{13}C NMR (DMSO, 63 MHz) δ_C = 25.5, 40.9, 44.0, 51.1, 58.2, 126.7, 127.1, 127.7, 130.2, 137.5, 138.6, 155.8, 174.3 ppm; MS (ES+): *m/z* 535, 519, 497, 287, 271, 249 $[M+H]^+$, 174; HPLC t_R = 11.4 min.

Moc-(*S*)-α-MeAba-Gly-O*t*Bu (15): NaH (333 mg, 14.4 mmol, 3.0 equiv) was added to a cooled solution of 4-(*S*)-methyloxycarbonylamino-4-methyl-1,2,4,5-tetrahydro-2-benzazepin-3-one (**14**; 1.2 g, 4.8 mmol, 1.0 equiv) in *N*,*N*-dimethylformamide (90 mL), followed by the addition after 20 min of *tert*-butyl-bromoacetate (3.1 mL, 19.2 mmol, 4.0 equiv). After 20 min the ice-bath was removed and the mixture was stirred for 1 h. The mixture was diluted with EtOAc (300 mL) and the organic phase was subsequently extracted with a saturated $NaHCO_3$ solution (3×230 mL) and H_2O (2×300 mL), dried ($MgSO_4$), filtered and evaporated. The product was purified by flash column chromatography (EtOAc/cyclohexane 2:5), to yield a colorless oil (800 mg, 46%): R_f = 0.47 (EtOAc); $[\alpha]_D$ = +23.6 (*c* = 1 in CH_2Cl_2); ^{1}H NMR (DMSO, 250 MHz) δ_H = 0.94 (s, 3H), 1.17 (s, 9H), 2.46 (d, *J* = 14.1 Hz, 1H), 3.43 (s, 3H, CH_3 Moc), 3.77 (d, 1H, Hα Gly, ^2J = 16.5 Hz), 3.93 (d, 1H, *J* = 13.9 Hz), 4.03 (d, *J* = 14.9 Hz, 1H), 4.16 (d, *J* = 16.7 Hz, 1H), 4.94 (d, *J* = 14.8 Hz, 1H), 7.10–7.21 (m, 4H), 7.64 ppm (s, 1H); ^{13}C NMR (DMSO, 63 MHz) δ_C = 26.2, 27.5, 41.5, 51.1, 51.9, 53.3, 58.9, 80.2, 126.6, 127.8, 129.8, 137.3, 137.7, 155.8, 168.3, 173.3 ppm; MS (ES+): *m/z* 401, 385, 363 $[M+H]^+$, 307, 289, 261; HPLC t_R = 15.5 min.

Boc-(*S*)-α-MeAba-Gly-OH (16): Moc-(*S*)-α-MeAba-Gly-O*t*Bu (**15**; 718 mg, 1.98 mmol, 1.0 equiv) was dissolved in HBr (33%) in AcOH (40 mL) and stirred at 55 °C for 1.5 h. The reaction mixture was evaporated and repeatedly redissolved in AcOH and evaporated, to yield brown oil of HBr·H-(*S*)-α-MeAba-Gly-OH (quantitative): R_f = 0.6 ($MeOH/CH_2Cl_2$); $[\alpha]_D$ = −7.1 (*c* = 1 in dioxane); ^{1}H NMR (DMSO, 250 MHz) δ_H = 1.89 (s, 3H), 3.13 (d, *J* = 14.6 Hz, 1H), 3.55 (d, *J* = 14.6 Hz, 1H), 4.15 (d, *J* = 17.2 Hz, 1H), 4.29 (d, *J* = 17.2 Hz, 1H), 4.56 (d, *J* = 15.1 Hz, 1H), 4.69 (d, *J* = 15.1 Hz, 1H), 7.25–7.41 (m, 4H), 8.43 ppm (s, 3H); ^{13}C NMR (DMSO, 63 MHz) δ_C = 25.0, 38.4, 51.8, 51.9, 59.3, 127.5, 128.5, 129.7, 135.3, 136.9, 170.1, 170.8 ppm; MS (ES+): *m/z* 249 $[M+H]^+$, 232, 204, 214; HPLC t_R = 9.1 min.

Et_3N (238 μL, 1.98 mmol, 1.0 equiv) and di-*tert*-butyldicarbonate (3.1 mL, 15.8 mmol, 8.0 equiv) were added to a cooled solution of HBr·NH_2-(*S*)-α-MeAba-Gly-OH (1.98 mmol) in dioxane/H_2O (17 mL, 9:1). After 30 min the pH was checked and adjusted to 9, if necessary. The reaction mixture was stirred, overnight, at room temperature. The solution was evaporated and the residue was redissolved in H_2O (20 mL), followed by adjustment of the pH to 3–4 with $KHSO_{4\,aq}$ (10%) solution in the presence of EtOAc (10 mL). The phases were separated and the aqueous layer was extracted with EtOAc (3×10 mL). The combined organic phases were dried ($MgSO_4$), filtered and evaporated and yielded compound **16** (460 mg, 67%): R_f = 0.55 (EtOAc/MeOH 49:49 + 2% AcOH); mp: 98.6–99.5 °C; $[\alpha]_D$ = +9.7 (*c* = 1 in CH_2Cl_2); ^{1}H NMR (DMSO, 250 MHz) δ_H = 1.26 (s, 3H), 1.45 (s, 9H), 2.72 (d, *J* = 14.3 Hz, 1H), 3.92–4.17 (m, 3H), 4.79 (d, *J* = 16.9 Hz, 1H), 5.24 (d, *J* = 14.5 Hz, 1H), 5.52 (br s, 1H), 7.24–7.35 ppm (m, 4H); ^{13}C NMR (DMSO, 63 MHz) δ_C = 26.3, 28.3, 42.3, 53.3, 53.9, 59.9, 127.5, 127.9, 129.0, 130.1,

136.4, 136.8, 156.4, 170.7, 175.1 ppm; MS (ES+): *m/z* 387, 371, 349 $[M+H]^+$, 293, 249, 235, 218; HPLC $t_R = 15.0$ min.

Peptides 5–8

H-Tyr-D-Ala-(*S*)-Aba-Gly-Tyr-Pro-Ser-NH_2·TFA (5): White powder, 25.0 mg, 45%; $R_f = 0.58$ (EBAW); HRMS-ES+: *m/z* $[M+H]^+$ calcd for $C_{41}H_{51}N_8O_{10}$: 816.3801, found: 816.3770; HPLC $t_R = 10.5$ min.

H-Tyr-D-Ala-(*R*)-Aba-Gly-Tyr-Pro-Ser-NH_2·TFA (6): White powder, 24.0 mg, 43%; $R_f = 0.63$ (EBAW); HRMS-ES+: *m/z* $[M+H]^+$ calcd for $C_{41}H_{51}N_8O_{10}$: 816.3801, found: 816.3811; HPLC; $t_R = 10.0$ min.

H-Tyr-D-Ala-(*S*)-MeAba-Gly]-Tyr-Pro-Ser-NH_2·TFA (7): White powder, 20.4 mg, 3%: $R_f = 0.43$ (EBAW); HRMS-ES+: *m/z* $[M+H]^+$ calcd for $C_{42}H_{53}N_8O_{10}$: 830.3958, found: 830.3930; HPLC $t_R =$ 10.42 min.

H-Tyr-D-Ala-(*R*)-MeAba-Gly]-Tyr-Pro-Ser-NH_2·TFA (8): White powder, 10.0 mg, 2%: $R_f = 0.40$. (EBAW); HRMS-ES+: *m/z* $[M+H]^+$ calcd for $C_{42}H_{53}N_8O_{10}$: 830.3958, found: 830.3955; HPLC $t_R =$ 10.73 min.

Acknowledgements

This work was supported by the Research Foundation, Flanders (FWO-Vlaanderen, Belgium, grant G.0008.08), the I.W.T. (Institute for the Promotion of Innovation by Science and Technology in Flanders, SBO-project IWT 040083) and the European grant "Normolife" (LSHC-CT-2006-037733).

Keywords: beta-turn stabilization · molecular dynamics · ligand design · ligand effects · opioid peptides

[1] B. L. Kieffer, *J. Pain* **2000**, *1*, 45–50.
[2] S. M. Johnson, W. W. Fleming, *Pharmacol. Rev.* **1989**, *41*, 435–488.
[3] V. J. Hruby, R. S. Agnes, *Biopolymers* **1999**, *51*, 391–410.
[4] P. C. Montecucchi, R. De Castiglioni, S. Piani, L. Gozzini, V. Erspamer, *Int. J. Pept. Protein Res.* **1981**, *17*, 275–283.
[5] M. Amiche, S. Sagan, A. Mor, A. Delfour, P. Nicolas, *Int. J. Pept. Prot. Res.* **1988**, *32*, 506–511.
[6] M. Broccardo, V. Erspamer, G. Falconieri-Erspamer, G. Improta, G. Linari, P. Melchiorri, P. C. Montecucchi, *Br. J. Pharmacol.* **1981**, *73*, 625–631.
[7] M. A. Castiglione-Morelli, F. Lelj, A. Pastore, S. Salvadori, T. Tancredi, R. Tomatis, E. Trivellone, P. A. Temussi, *J. Med. Chem.* **1987**, *30*, 2067–2073.
[8] M. M. Słabicki, M. J. Potrzebowski, G. Bujacz, S. Olejniczak, J. Olczak, *J. Phys. Chem. B* **2004**, *108*, 4535–4545.
[9] A. Pastore, P. A. Temussi, T. Tancredi, S. Salvadori, R. Tomatis, *Biopolymers* **1984**, *23*, 2349–2360.
[10] P. A. Temussi, D. Picone, T. Tancredi, R. Tomatis, S. Salvadori, M. Marastoni, G. Balboni, *FEBS Lett.* **1989**, *247*, 283–288.
[11] G. Balboni, M. Marastoni, D. Picone, S. Salvadori, T. Tancredi, P. A. Temussi, R. Tomatis, *Biochem. Biophys. Res. Commun.* **1990**, *169*, 617–622.
[12] T. Tancredi, P. A. Temussi, D. Picone, P. Amodeo, R. Tomatis, S. Salvadori, M. Marastoni, V. Santagada, G. Balboni, *Biopolymers* **1991**, *31*, 751–760.
[13] M. A. Castiglione-Morelli, T. Tancredi, E. Trivellone, G. Balboni, M. Marastoni, S. Salvadori, R. Tomatis, P. A. Temussi, *Biopolymers* **1988**, *27*, 1353–1361.
[14] B. C. Wilkes, P. W. Schiller, *Biopolymers* **1990**, *29*, 89–95.
[15] M. D. Shenderovich, G. V. Nikiforovich, A. A. Golbraikh, *Int. J. Pept. Prot. Res.* **1991**, *37*, 241–251.
[16] P. Amodeo, A. Motta, T. Tancredi, S. Salvadori, R. Tomatis, D. Picone, G. Saviano, P. A. Temussi, *Pept. Res.* **1992**, *5*, 48–55.
[17] D. Tourwe, K. Verschueren, A. Frycia, P. Davis, F. Porreca, V. J. Hruby, G. Toth, H. Jaspers, P. Verheyden, G. VanBinst, *Biopolymers* **1996**, *38*, 1–12.
[18] D. Tourwé, K. Verschueren, G. VanBinst, P. Davis, F. Porreca, V. J. Hruby, *Bioorg. Med. Chem. Lett.* **1992**, *2*, 1305–1308.
[19] S. Ballet, A. Frycia, J. Piron, N. N. Chung, P. W. Schiller, P. Kosson, A. W. Likpowski, D. Tourwé, *J. Pept. Res.* **2005**, *66*, 222–230.
[20] K. Van Rompaey, S. Ballet, C. Tomboly, R. De Wachter, K. Vanommeslaeghe, M. Biesemans, R. Willem, D. Tourwé, *Eur. J. Org. Chem.* **2006**, 2899–2911.
[21] R. De Wachter, L. Brans, S. Ballet, I. Van den Eynde, D. Feytens, A. Keresztes, G. Toth, Z. Urbanczyk-Lipkowska, D. Tourwé, *Tetrahedron* **2009**, *65*, 2266–2278.
[22] C. Bisang, C. Weber, J. Inglis, C. A. Schiffer, W. F. van Gunsteren, I. Jelesarov, H. R. Bosshard, J. A. Robinson, *J. Am. Chem. Soc.* **1995**, *117*, 7904–7915.
[23] A. Flores-Ortega, A. I. Jimenez, C. Cativiela, R. Nussinov, C. Aleman, J. Casanovas, *J. Org. Chem.* **2008**, *73*, 3418–3427.
[24] M. J. O'Donnell, W. D. Bennett, S. D. Wu, *J. Am. Chem. Soc.* **1989**, *111*, 2353–2355.
[25] M. J. O'Donnell, S. D. Wu, J. C. Huffman, *Tetrahedron* **1994**, *50*, 4507–4518.
[26] E. J. Corey, F. Xu, M. C. Noe, *J. Am. Chem. Soc.* **1997**, *119*, 12414–12415.
[27] B. Lygo, P. G. Wainwright, *Tetrahedron Lett.* **1997**, *38*, 8595–8598.
[28] T. Ooi, M. Kameda, K. Maruoka, *J. Am. Chem. Soc.* **1999**, *121*, 6519–6520.
[29] E. J. Corey, M. C. Noe, F. Xu, *Tetrahedron Lett.* **1998**, *39*, 5347–5350.
[30] B. Lygo, J. Crosby, J. A. Peterson, *Tetrahedron Lett.* **1999**, *40*, 1385–1388.
[31] M. J. O'Donnell, S. D. Wu, *Tetrahedron: Asymmetry* **1992**, *3*, 591–594.
[32] B. Lygo, J. Crosby, J. A. Peterson, *Tetrahedron Lett.* **1999**, *40*, 8671–8674.
[33] R. Chinchilla, C. Najera, F. J. Ortega, *Eur. J. Org. Chem.* **2007**, 6034–6038.
[34] T. Ooi, M. Takeuchi, M. Kameda, K. Maruoka, *J. Am. Chem. Soc.* **2000**, *122*, 5228–5229.
[35] K. Maruoka, *J. Fluorine Chem.* **2001**, *112*, 95–99.
[36] S. S. Jew, B. S. Jeong, J. H. Lee, M. S. Yoo, Y. J. Lee, B. S. Park, M. G. Kim, H. G. Park, *J. Org. Chem.* **2003**, *68*, 4514–4516.
[37] S. S. Jew, M. S. Yoo, B. S. Jeong, I. Y. Park, H. G. Park, *Org. Lett.* **2002**, *4*, 4245–4248.
[38] M. S. Yoo, B. S. Jeong, J. H. Lee, H. G. Park, S. S. Jew, *Org. Lett.* **2005**, *7*, 1129–1131.
[39] M. Kitamura, S. Shirakawa, K. Maruoka, *Angew. Chem.* **2005**, *117*, 1573–1575; *Angew. Chem. Int. Ed.* **2005**, *44*, 1549–1551.
[40] E. Olajos, A. Péter, R. Casimir, D. Tourwé, *Chromatographia* **2001**, *54*, 77–82.
[41] U. Schöllkopf, W. Hartwig, U. Groth, K. O. Westphalen, *Liebigs Ann. Chem.* **1981**, 696–708.
[42] U. Schöllkopf, *Tetrahedron* **1983**, *39*, 2085–2091.
[43] R. M. Williams, M. N. Im, *J. Am. Chem. Soc.* **1991**, *113*, 9276–9286.
[44] D. Seebach, A. Fadel, *Helv. Chim. Acta* **1985**, *68*, 1243–1250.
[45] S. Karady, J. S. Amato, L. M. Weinstock, *Tetrahedron Lett.* **1984**, *25*, 4337–4340.
[46] A. B. Smith III, R. C. Holcomb, M. C. Guzman, T. P. Keenan, P. A. Sprengeler, R. Hirschmann, *Tetrahedron Lett.* **1993**, *34*, 63–66.
[47] F. Alonso, S. G. Davies, A. S. Elend, J. L. Haggitt, *J. Chem. Soc. Perkin Trans. 1* **1998**, 257–264.
[48] K. Nebel, M. Mutter, *Tetrahedron* **1988**, *44*, 4793–4796.
[49] S. R. Kapadia, D. M. Spero, M. Eriksson, *J. Org. Chem.* **2001**, *66*, 1903–1905.
[50] D. M. Coe, R. Perciaccante, P. A. Procopiou, *Org. Biomol. Chem.* **2003**, *1*, 1106–1111.
[51] S. Vassiliou, P. A. Magriotis, *Tetrahedron: Asymmetry* **2006**, *17*, 1754–1757.
[52] a) S. A. Krumins, *Neuropeptides* **1987**, *9*, 93–102; b) M. Amiche, S. Sagan, A. Mor, A. Delfour, P. Nicolas, *Int. J. Pept. Protein Res.* **1988**, *32*, 506–511; c) M. Amiche, S. Sagan, A. Mor, D. Pelaprat, W. Rostene, A. Delfour, P. Nicolas, *Eur. J. Biochem.* **1990**, *189*, 625–635.
[53] J. R. Maple, U. Dinur, A. T. Hagler, *Proc. Natl. Acad. Sci. USA* **1988**, *85*, 5350–5354.
[54] C. Tömböly, S. Ballet, D. Feytens, K. E. Köver, A. Borics, S. Lovas, M. Al-Khrasani, Z. Fürst, G. Toth, S. Benyhe, D. Tourwé, *J. Med. Chem.* **2008**, *51*, 173–177.
[55] A. Madder, N. Farcy, N. G. C. Hosten, H. De Muynck, P. J. De Clercq, J. Barry, A. P. Davis, *Eur. J. Org. Chem.* **1999**, 2787–2791.
[56] A. Keresztes, M. Szücs, A. Borics, E. K. Kövér, E. Forró, F. Fülöp, C. Tömböly, A. Péter, A. Páhi, G. Fábián, M. Murányi, G. Tóth, *J. Med. Chem.* **2008**, *51*, 4270–4279.

[57] M. M. Bradford, *Anal. Biochem.* **1976**, *72*, 248 – 254.
[58] G. Fábián, B. Bozó, M. Szikszay, G. Horváth, C. J. Coscia, M. Szűcs, *J. Pharmacol. Exp. Ther.* **2002**, *302*, 774 – 780.
[59] S. Berger, S. Braun, *200 and more NMR experiments*, Wiley-VCH, Weinheim, **2004**, and references therein.
[60] N. Birlirakis, P. Berthault, H. Desvaux, M. Goldman, *Bruker Report* **1996**, *142*, 34 – 38.
[61] W. F. Vranken, W. Boucher, T. J. Stevens, R. H. Fogh, A. Pajon, P. Llinas, E. L. Ulrich, J. L. Markley, J. Ionides, E. D. Laue, *Proteins Struct. Funct. Bioinf.* **2005**, *59*, 687 – 696.
[62] D. Neuhaus, M. P. Williamson, *The Nuclear Overhauser Effect in Structural and Conformational Analysis, 2 ed.*, Wiley-VCH, Weinheim, **2000**.
[63] S. Kirkpatrick, C. D. Gelatt, M. P. Vecchi, *Science* **1983**, *220*, 671 – 680.
[64] V. Černý, *J. Optimiz. Theory App.* **1985**, *45*, 41 – 51.
[65] a) A. E. Torda, R. M. Scheek, W. F. van Gunsteren, *Chem. Phys. Lett.* **1989**, *157*, 289 – 294; b) A. P. Nanzer, W. F. van Gunsteren, A. E. Torda, *J. Biomol. NMR* **1995**, *6*, 313 – 320; c) D. A. Pearlman, *J. Biomol. NMR* **1994**, *4*, 1 – 16; d) P. M. S. Hendrickx, F. Corzana, S. Depraetere, D. A. Tourwé, K. Augustyns, J. C. Martins, *J. Comput. Chem.* **2010**, *31*, 561 – 572.
[66] D. A. Case, T. A. Darden, I. T. E. Cheatham, C. L. Simmerling, J. Wang, R. E. Duke, R. Luo, K. M. Merz, D. A. Pearlman, M. Crowley, R. C. Walker, W. Zhang, B. Wang, S. Hayik, A. Roitberg, G. Seabra, K. F. Wong, F. Paesani, X. Wu, S. Brozell, V. Tsui, H. Gohlke, L. Yang, C. Tan, J. Mongan, V. Hornak, G. Cui, P. Beroza, D. H. Mathews, C. Schafmeister, W. S. Ross, P. A. Kollman, AMBER 9, University of California, San Francisco, **2006**.
[67] J. Wang, R. M. Wolf, J. W. Caldwell, P. A. Kollman, D. A. Case, *J. Comput. Chem.* **2004**, *25*, 1157 – 1174.
[68] a) A. Jakalian, B. L. Bush, D. B. Jack, C. I. Bayly, *J. Comput. Chem.* **2000**, *21*, 132 – 146; b) A. Jakalian, D. B. Jack, C. I. Bayly, *J. Comput. Chem.* **2002**, *23*, 1623 – 1641.

Received: June 28, 2011
Published online on August 29, 2011

